

# Laser cladding of high-entropy alloy on H13 steel

Xiao-Tao Liu\*, Wen-Bin Lei, Jie Li,  
Yu Ma, Wei-Ming Wang, Bao-Hua Zhang,  
Chang-Sheng Liu, Jian-Zhong Cui

Received: 23 August 2013/Revised: 16 January 2014/Accepted: 25 June 2014/Published online: 6 November 2014  
© The Nonferrous Metals Society of China and Springer-Verlag Berlin Heidelberg 2014

**Abstract** High-entropy alloy layer up to 150  $\mu\text{m}$  in thickness was formed on H13 substrate with a metallurgical bonding at the coating/substrate interface. Simple solid solution phases were formed in the coating layer with a typical microstructure composed of both dendrite and interdendrite. The microstructure at the top of the cladding zone consists of equiaxed grains while that at the bottom consists of columnar grains. The coating layer exhibits great enhancement in microhardness and wear resistance compared with the H13 substrate.

**Keywords** Laser cladding; High-entropy alloy; Microhardness; Wear rate

## 1 Introduction

High-entropy alloys (HEAs) developed by Yeh et al. [1], in 1995 is a novel alloy system which consists of at least five principal elements in equiatomic or close-to-equiatomic ratios. In this highly concentrated multi-components alloy systems, simple solid solutions with FCC and/or BCC structure rather than complex intermetallics tend to form, partly due to the significant entropic contribution which lowers the Gibbs energy of the solid solution, especially at elevated temperatures [2]. The simple solid solution

microstructure after solidification imparts the HEAs excellent mechanical and chemical properties such as high hardness and mechanical strength, good wear, corrosion and oxidation resistance [3–5]. Thus, it is anticipated that the HEAs could have a great potential in hard-facing applications where high hardness and good wear resistance are required.

Laser cladding (LC) is an efficient approach for manufacturing various surface coatings with a significant thickness to ensure that the surface properties can be tailored to impart excellent wear, corrosion and oxidation resistance to combat virtually any degradation while the bulk substrate remains unaffected [6–9]. For LC, the design and development of powder materials are the key to produce high-performance coatings. Here, this study aims to evaluate the possibility of synthesizing HEA layer by LC technique on the surface of a hot-work tool steel plank. The HEA cladding layer was evaluated according to its microstructure, hardness and the high-temperature wear performance.

## 2 Experimental

H13 steel planks (40 mm  $\times$  15 mm  $\times$  10 mm) were used as the substrate materials. The elemental powders of Al, Co, Cr, Cu, Fe, Ni with purity higher than 99.9 % were well mixed in atomic ratio of  $\text{Al}_2\text{CoCrCuFeNi}$  as the raw material. Before LC, the substrates were ultrasonic-cleaned in acetone and polished to obtain uniform roughness. The powder materials were mixed uniformly with an organic binder and pre-placed onto the substrates. After coating, specimens were dried in air for 2 days, and the dried coating was ground to a thickness of 1 mm by 1,000 grade SiC paper in dry condition. A pulsed Nd:YAG laser (JHM-

X.-T. Liu\*, W.-B. Lei, J. Li, Y. Ma, J.-Z. Cui  
The Key Laboratory of Electromagnetic Processing of Materials,  
Ministry of Education, Northeastern University,  
Shenyang 110819, China  
e-mail: lxtandm@gmail.com

W.-M. Wang, B.-H. Zhang, C.-S. Liu  
School of Materials and Metallurgy, Northeastern University,  
Shenyang 110819, China

1GY-400) with a maximum power of 400 W was used to re-melt the pre-placed layer by the relative movement between laser beam and the substrate. Argon gas blowing through a 4 mm diameter jet, coaxial with the laser beam, was used to shield the melt pool from oxidation and protect the laser optics from fumes and spattered particles. In the experiment, the current and scanning speed varied from 250 to 290 A and 1 to 7 mm·s<sup>-1</sup>, respectively. The defocus was fixed at -14 mm, while a 40 % track overlapping condition was used.

X-ray diffraction (XRD) was used for the identification of the crystal structure, and the scanning was performed at a  $2\theta$  range of 20°–100°. The microstructure and chemical composition of the cladding layer were examined using a scanning electron microscopy (SEM) equipped with energy dispersive X-ray spectrometer (EDX) and transmission electron microscope (TEM). The microhardness was measured using Vickers hardness tester under a load of 0.5 N for 10 s. In order to evaluate the high-temperature wear performance, the cladding specimens were tested at 500 °C using a pin-on-disk tribometer. The substrate was also tested as a reference material.

### 3 Results and discussions

The XRD pattern of the crystal structure of the coating layer is shown in Fig. 1. It reveals that the coating layer consists of FCC simple solid solution phase. Previous studies indicate that the Al<sub>x</sub>CoCrCuFeNi alloy system has a gradual microstructure change from FCC to BCC with aluminum content increasing [2]. With a small addition of aluminum ( $x \leq 0.8$ ), the alloys mainly consist of a simple FCC solid solution structure. As  $x$  increases to larger than 1.0, the alloys consist of single BCC solid solution phase. In this study, the formation of the FCC solid solution phase in the coating layer is due to the deviation of compositions,

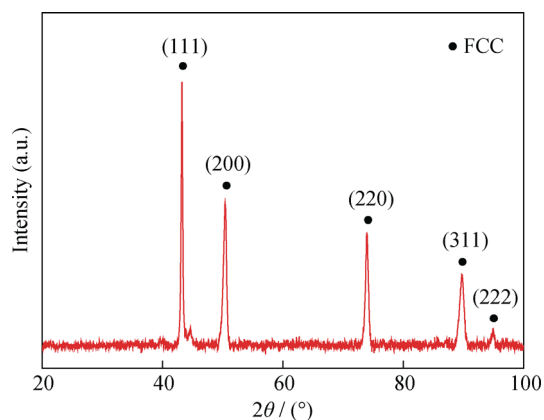


**Fig. 1** XRD pattern of laser cladding coating

especially Al and Fe, from the nominal one caused by the evaporation of Al and the dilution of Fe into the cladding layer from the substrate during LC, respectively. Among the components of the Al–Co–Cr–Cu–Fe–Ni HEA system, Al is a strong BCC former and Fe has no effect on the crystal structure [10, 11]. Thus, the decrease of Al due to evaporation during LC results in the occurrence of FCC solid solution phase instead of BCC phase, which is consistent with the EDS analysis hereafter.

The HEA coating layer in Fig. 2a consists of cladding zone (Fig. 2b, c), bounding zone and heat affected zone (Fig. 2d). The good fusion bond at the coating/substrate interface indicates that a metallurgical bond is obtained. The typical microstructures in the cladding zone consist of both dendrite and interdendrite. The top of the cladding zone mainly consists of equiaxed grains, and the bottom of the cladding zone consists of columnar grains. The high-temperature gradient at the bonding area of the coating causes a rapid directional solidification, and thus the growth direction of columnar grains is perpendicular to the interface. With the temperature gradient decreasing to the top of the coating, the columnar grains transform to equiaxed grains. As further confirmed by the TEM bright-field image and the corresponding selected area diffraction (SAD) pattern shown in Fig. 3a, both the dendrites and the interdendrites of the cladding layers presented in Fig. 2 consist of FCC structure. An ordered FCC phase (bright spots) is revealed by the SAD pattern and several nano-sized precipitates appear in the matrix during solidification, as shown in the TEM dark-field image in Fig. 3b.

The dendrite and interdendrite were analyzed by EDS and the following values are obtained: Al, 10.17 %; Co, 11.56 %; Cr, 14.55 %; Cu, 6.63 %; Fe, 45.36 %; Ni, 11.73 % for dendrite and Al, 12.37 %; Co, 4.64 %; Cr,

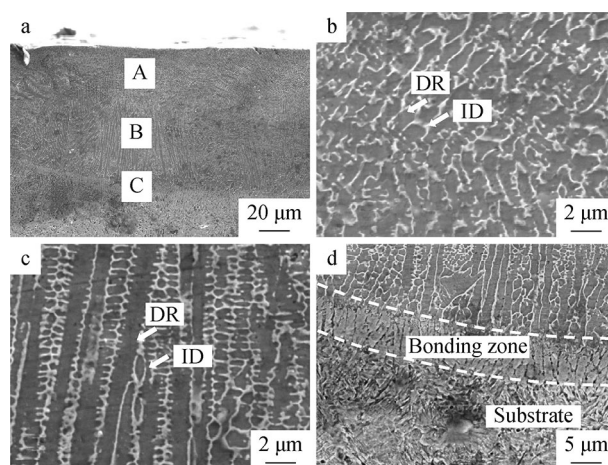


**Fig. 2** SEM images of high-entropy alloy layer by laser cladding: **a** cross-sectional microstructure and **b**, **c** and **d** magnification of Areas A, B and C in **a**

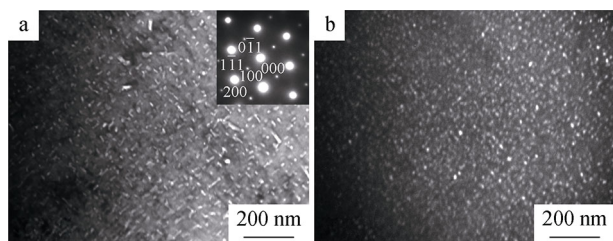


**Fig. 3** TEM images of dendrite of cladding layer: **a** bright-field image with SAD pattern of FCC [011] zone axis and **b** dark-field image corresponding to (100) superlattice spot of SAD pattern in **a**

2.56 %; Cu, 63.80 %; Fe, 7.30 %; and Ni, 9.33 % for the interdendrite. Cu element is enriched in the interdendritic structure, and the content of Cu element is up to more than 50 at %. The segregation of composition in HEAs depends on the mixing enthalpy because of the difference in their electronegativities among the principal components. The atomic pair with mixing enthalpy near zero can possess high solid solubility [12]. Cu has much more positive enthalpy with Fe compared with the other components, and thus it is excluded from the dendrites and enriched in interdendrites. The higher Fe content than the nominal one results from the dilution of the cladding layer by the H13 substrate, and the lower Al content than the nominal one may come from the burning and evaporation of Al powders due to the low melting point of Al.

Figure 4 shows the microhardness distribution ranging from surface of the coating to H13 substrate, and the insert represents a typical cross-sectional microstructure of the coated specimen. The hardness values measured for the HEA coating with the depth of 150  $\mu\text{m}$  range between HV 402 and HV 497. The microhardness indicates a gradient distribution from cladding HEA coating to H13 substrate. The average microhardness of the coating layer shows  $\sim 70\%$  enhancement compared with that ( $\sim \text{HV } 250$ ) of the H13 substrate. Regarding wear resistance, the average weight losses of the uncoated and the laser coated specimens after the pin-on-disk wear test at 500  $^{\circ}\text{C}$  are found to be 29.8 and 9.7 mg, respectively. Figure 5 shows the correlation between the wear rate and the microhardness of the specimens without and with HEA coating in the pin-on-disk test. The wear rate of the coated sample is 30 % that of the H13 substrate, indicating that the HEA coating exhibits significantly enhanced resistance to wear. The insets in Fig. 5 show the morphologies of the worn surface after test. Obvious differences in wear surface morphology are seen between the specimens without and with HEA coating. For the substrate without coating, the worn surface is grooved, significant ductile deformation along the groove is seen, and cracks also exist in the worn surface. It is indicated that the adhesive wear of the substrate at 500  $^{\circ}\text{C}$  is

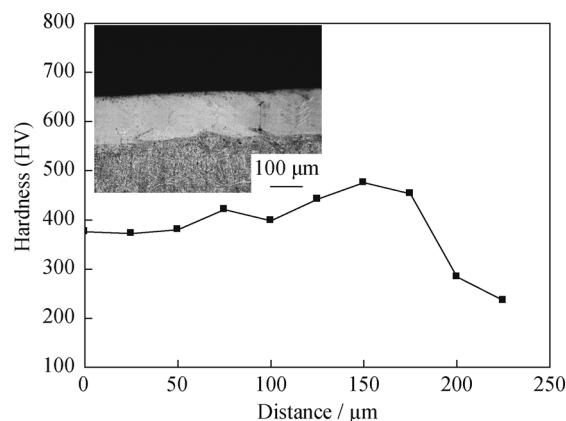


**Fig. 4** Microhardness distribution ranging from surface of HEA coating to H13 substrate (insert representing a typical cross-sectional OM image of coated specimens)

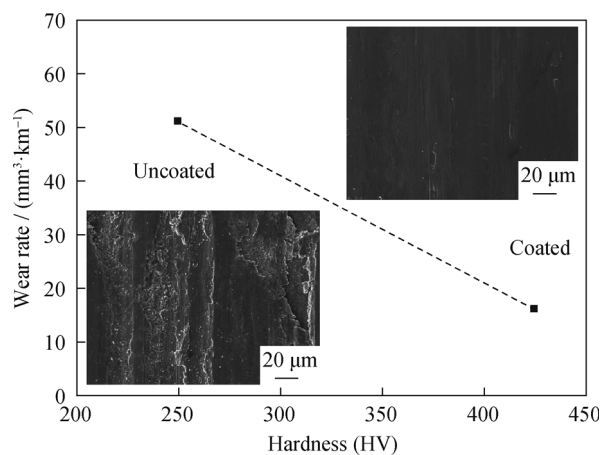


**Fig. 5** Correlation between wear rate and microhardness of specimens without and with HEA coating (inserts representing SEM images of worn surface of specimens without and with HEA coating)

predominantly of delamination by which the worn surface undergoes a periodic fracture [13, 14]. For the HEA coated specimens, the surface is much smoother with fewer shallow grooves, indicating a great enhancement of wear resistance due to the higher hardness which resists plastic deformation and delamination is obtained.

Zhu et al. [15] investigated the effect of carbon on Al-CoCrFeNi alloy and found carbon existed mainly in the form of carbonization or free carbon. The strength and ductility of the alloys were degraded due to the inhomogeneously distributed brittle  $\epsilon$  phase and graphite in the alloy. In this study, it was supposed that the dilution of carbon into the cladding layer from the substrate would occur. However, there are no carbides and/or free carbon detected in the cladding layer. Thus, the effect of carbon is

minor and the improved hardness and wear resistance of the cladding are principally due to the formation of HEA by LC on the H13 substrate.

#### 4 Conclusions

HEA coating layer with FCC simple solid solution structure was successfully fabricated on the H13 substrate with a depth of 150  $\mu\text{m}$ . A good metallurgical bond without any porosity or cracks is obtained at the substrate/coating interface. The surface hardness and high-temperature wear resistance of H13 substrate are significantly improved by cladding with the HEA.

**Acknowledgments** This work was financially supported by the National Natural Science Foundation of China (No. 50401006), the Fundamental Research Funds for the Central Universities (No. N120409003) and the University Students' Innovation Plan of China (No. 130066).

#### References

- [1] Yeh JW, Chen YL, Lin SJ, Chen SK. High-entropy alloys—a new era of exploitation. *Mater Sci Forum*. 2007;560:1.
- [2] Yeh JW, Chen SK, Lin SJ, Gan JY, Chin TS, Shun TT, Tsau CH, Chang SY. Nanostructured high-entropy alloys with multiple principal elements: novel alloy design concepts and outcomes. *Adv Eng Mater*. 2004;6(5):299.
- [3] Zhou YJ, Zhang Y, Kim TN, Chen GL. Microstructure characterizations and strengthening mechanism of multi-principal component AlCoCrFeNiTi<sub>0.5</sub> solid solution alloy with excellent mechanical properties. *Mater Lett*. 2008;62(17–18):2673.
- [4] Chen YY, Duval T, Hung UD, Yeh JW, Shih HC. Microstructure and electrochemical properties of high entropy alloys—a comparison with type-304 stainless steel. *Corros Sci*. 2005;47(9):2257.
- [5] Wu JM, Lin SJ, Yeh JW, Chen SK, Huang YS, Chen HC. Adhesive wear behavior of Al<sub>x</sub>CoCrCuFeNi high-entropy alloys as a function of aluminum content. *Wear*. 2006;261(5–6):513.
- [6] Zhao HB, Tu HL, Wei F, Zhang XQ, Xiong YH, Du J. Resistive switching characteristics of Dy<sub>2</sub>O<sub>3</sub> film with a Pt nanocrystal embedding layer formed by pulsed laser deposition. *Rare Met*. 2014;33(1):75.
- [7] Yang S, Chen N, Liu WJ, Zhong ML. In situ formation of MoSi<sub>2</sub>/SiC composite coating on pure Al by laser cladding. *Mater Lett*. 2003;57(22–23):3412.
- [8] Yue TM, Li T, Lin X. Microstructure and phase evolution in laser cladding of Ni/Cu/Al multilayer on magnesium substrate. *Metall Mater Trans A*. 2010;41(1):212.
- [9] Yun CL, Zhang QL, Luo XF, Zhang ZR. Formation and strain distribution of Ni/NiO core/shell magnetic nanoparticles fabricated by pulsed laser deposition. *Sci China Phys Mech Astron*. 2011;54(7):1254.
- [10] Tong CJ, Chen YL, Chen SK, Yeh JW, Shun TT, Tsau CH, Lin SJ, Chang SY. Microstructure characterization of Al<sub>x</sub>CoCrCuFeNi high-entropy alloy system with multiprincipal elements. *Metall Mater Trans A*. 2004;36(4):881.
- [11] Ren B, Liu ZX, Li DM, Shi L, Cai B, Wang MX. Effect of elemental interaction on microstructure of CuCrFeNiMn high entropy alloy system. *J Alloy Compd*. 2010;493(1–2):148.
- [12] Tung CC, Yeh JW, Shun TT, Chen SK, Huang YS, Chen HC. On the elemental effect of AlCoCrCuFeNi high-entropy alloy system. *Mater Lett*. 2007;61(1):1.
- [13] Wu XF, Zhang GG, Wu FF. Microstructure and dry sliding wear behavior of cast Al–Mg<sub>2</sub>Si in situ metal matrix composite modified by Nd. *Rare Met*. 2013;32(3):284.
- [14] Wu JM, Lin SJ, Yeh JW, Chen SK, Huang YS, Chen HC. Adhesive wear behavior of Al<sub>x</sub>CoCrCuFeNi high-entropy alloys as a function of aluminum content. *Wear*. 2006;261(5–6):513.
- [15] Zhu JM, Fu HM, Zhang HF, Wang AM, Li H, Hu ZQ. Microstructure and compressive properties of multiprincipal component AlCoCrFeNiC<sub>x</sub> alloys. *J Alloy Compd*. 2011;509(8):3476.